A Predictive Model for Blood-Brain Barrier Penetration

Xuchun Fu,[1,*] Zhifang Song,[2] Wenquan Liang[3]

[1] Department of Pharmacy, Zhejiang University City College, Hangzhou, P.R.China
[2] College of Medicine, Zhejiang University, Hangzhou, P.R.China
[3] College of Pharmaceutical Sciences, Zhejiang University, Hangzhou, P.R.China

Abstract

Motivation. It is important to determine whether a candidate molecule is capable of penetrating the blood-brain barrier in drug discovery and development. The aim of this paper is to establish a predictive model for blood-brain barrier penetration only using two simple descriptors, molecular volume and polar surface area.

Method. A dataset of 111 compounds is divided into a training set of 86 compounds and a test set of 25 compounds. Molecular volumes and polar surface areas are obtained from the molecular conformations optimized using the semiempirical self-consistent field molecular orbital calculation AM1 method. The model to predict blood-brain barrier penetration from molecular volume and polar surface area is derived on the training set using the stepwise multiple regression analysis and then cross-validated using leave-one-out procedure and tested on the external prediction.

Results. The logarithm of the ratio of the steady-state concentration of a compound in the brain to in the blood, log*BB*, is correlated with its molecular volume parabolically and its polar surface area inversely. Both calculated log*BB* values for the training set and predicted log*BB* values for the test set are in good agreement with respective experimental ones.

Conclu*sions. The model derived in this paper appears to be very simple but robust and effective for predictive use, so it is suitable for the rapid prediction of the blood-brain barrier penetration for a wide range of drug candidates.

Keywords. Blood-brain barrier; predictive model; molecular volume; polar surface area

Abbreviations and notations

BBB, blood-brain barrier	BB, brain/blood concentration ratio
CNS, central nervous system	V, molecular volume
PSA, polar surface area	RMSE, root mean square error

1 INTRODUCTION

It is important to determine whether a candidate molecule is capable of penetrating the blood-brain barrier (BBB) in drug discovery and development. Drugs that act in the central nervous system (CNS) need to cross the BBB to reach their molecular target. By contrast, for drugs with a peripheral target, little or no BBB penetration

* Correspondence author; Email: fuxc@zucc.edu.cn; Phone: 86-571-88018711; Fax: 86-571-88018441

might be required in order to avoid or minimize CNS side effects. A common measure of the degree of BBB penetration is the ratio of the steady-state concentration of the drug molecule in the brain to in the blood, usually expressed as $\log(C_{brain/blood})$ or log*BB*. The experimental determination of log*BB* is a time-consuming, expensive, and difficult technique, requiring animal experiments and the synthesis of the test compounds, usually in radiolabeled form [1-4]. It is of considerable value to predict log*BB* values of compounds from their physicochemical parameters or, ideally, from their molecular structures.

Young et al. [2] showed that log*BB* values of 20 H_2 receptor histamine antagonists were correlated with $\Delta\log P$ (octanol-cyclohexane). van de Waterbeemd and Kansy [5] examined the same series of 20 compounds and found a significant correlation between log*BB* and the cyclohexane-water partition coefficient when the molecular volume was included in the parameterization. They also found that log*BB* was correlated with polar surface area (*PSA*, defined as the sum of the van der Waals surface areas of oxygen atoms, nitrogen atoms, and attached hydrogen atoms in a molecule), but the model showed it to be poorly predictive when tested with compounds outside its training set [6], suggesting that the structural diversity of the 20 H_2 receptor histamine antagonists might be insufficient to develop a generally applicable model for predicting log*BB*. Thus Abraham et al. [7] constructed a larger training set of 65 compounds and derived a correlation between log*BB* and solvato-chromatic parameters for 57 compounds (8 compounds were excluded as outliers). With a set of 57 compounds drawn from the Abraham training set mentioned above, Lombardo [8], Norinder [9], Clark [10] , and their co-workers developed the models for log*BB* prediction using calculated molecular structural parameters such as free energy of solvation in water, ΔG_w^0 [8], Molsurf parameters [9], *PSA*, and calculated octanol-water partition coefficient, Clog*P* or Mlog*P* [10], respectively. More recently, a variety of models to predict BBB penetration for larger dataset have been developed [11-16] using different descriptors such as the three-dimensional molecular field descriptors, electropological state indices, and so on. In summary, the BBB penetration of a compound is thought to be dependent on its hydrogen-bonding potential, lipophilicity and size. Weak hydrogen-bonding potential, high lipophilicity, and small size are favorable to BBB penetration.

In this paper, we derive a predictive model for BBB penetration only using two simple descriptors, molecular volume and polar surface area.

2 METHODS

The dataset of 111 compounds and their corresponding log*BB* values is taken from the literatures [2, 6-8, 17-22]. These compounds are divided into a training set of 86 compounds and a test set of 25 compounds. Molecular volumes and polar surface areas are selected as the structural descriptors to develop predictive model for BBB penetration. These structural descriptors are obtained from the molecular conformations optimized using the semiempirical self-consistent field molecular orbital calculation AM1 method [23] and the atomic radii used by Clark [10]. The model to predict blood-brain barrier penetration is derived on the training set using the stepwise multiple regression analysis and then cross-validated using leave-one-out procedure [24] in which

one compound is left out from the training set and predicted from the model based on the remaining data and tested on the external prediction.

3 RESULTS AND DISCUSSION

3.1 The Predictive Model of BBB Penetration only Including *V* and *PSA*

The 86 compounds of training set are illustrated in Figure1 and listed in Table 1 along with their experimental log*BB* values.

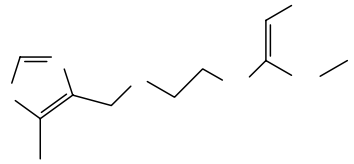

1

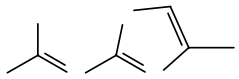

2

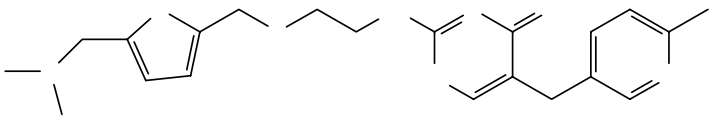

3

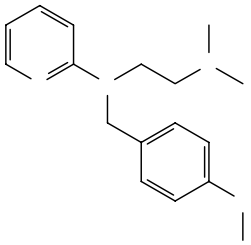

4

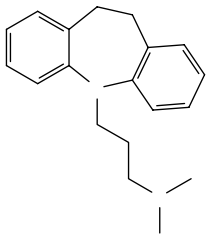

5

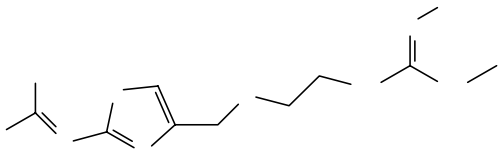

6

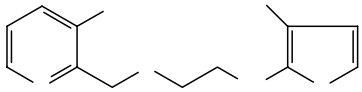

7

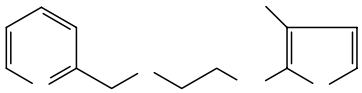

8

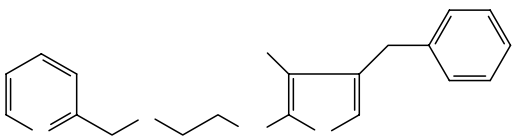

9

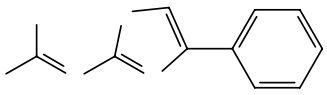

10

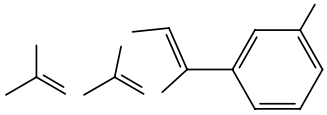

11

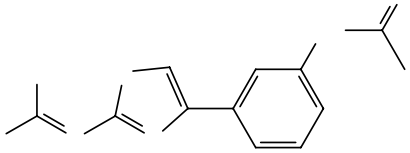

12

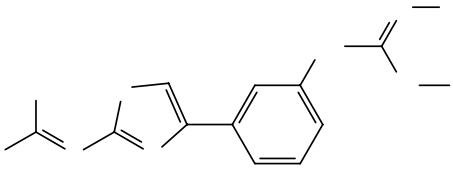

13

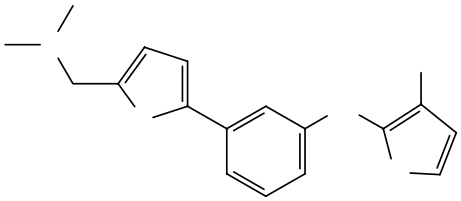

14

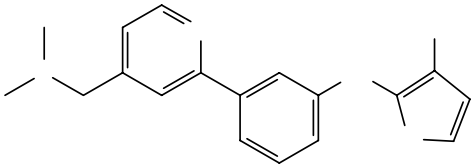

15

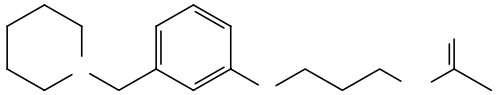

16

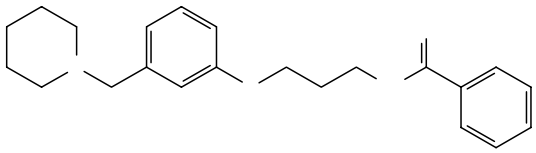

17

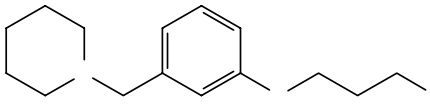

18

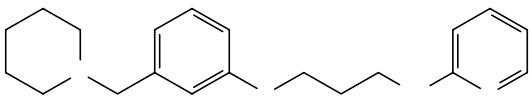

19

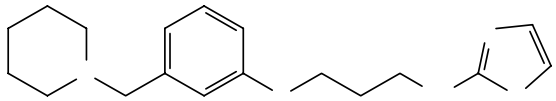

20

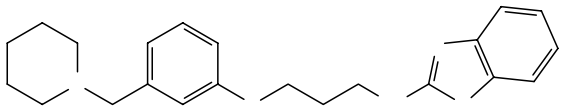

21

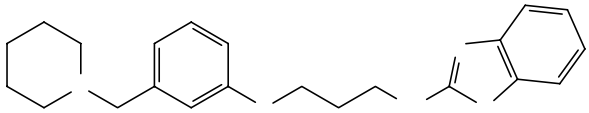

22

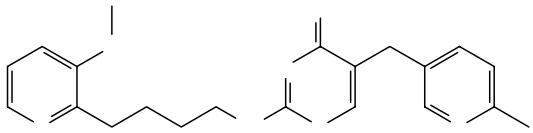

23

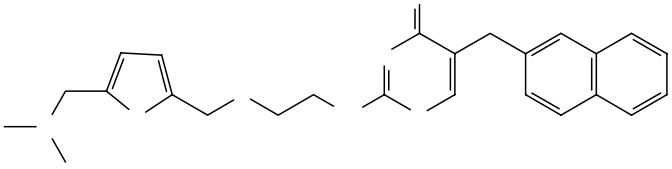

24

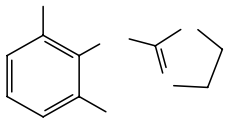

25

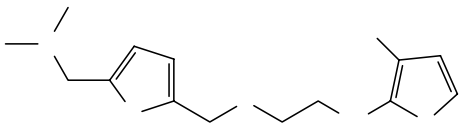

26

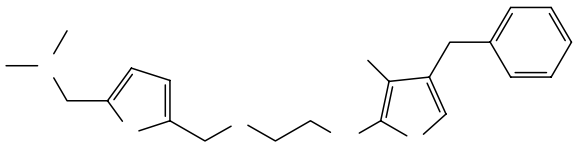

27

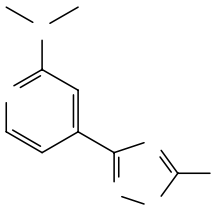

28

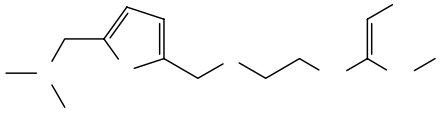

29

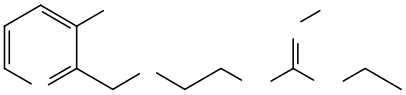

30

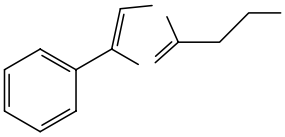

61

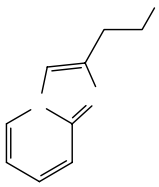

62

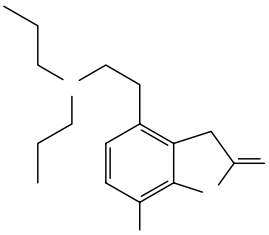

63

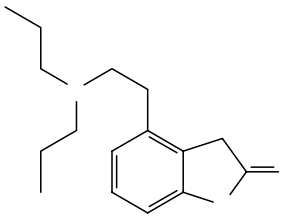

64

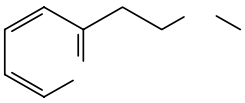

65

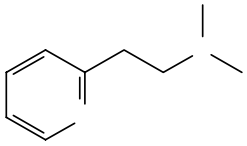

66

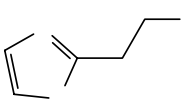

67

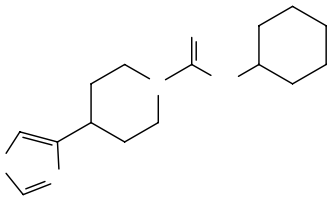

68

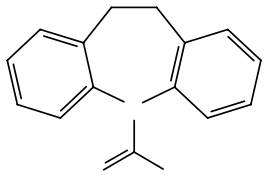

69

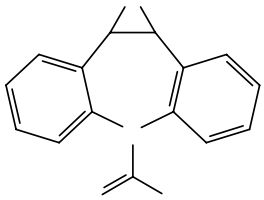

70

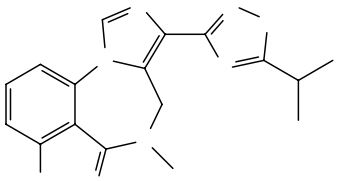

71

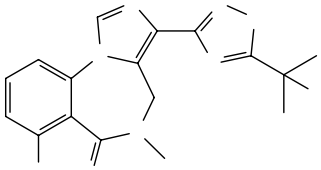

72

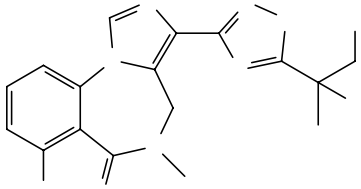

73

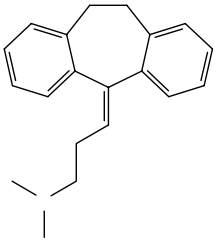

74

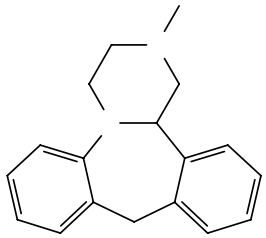

75

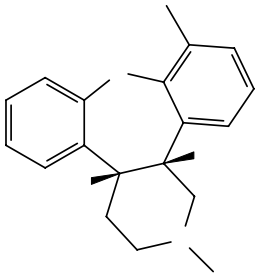

76

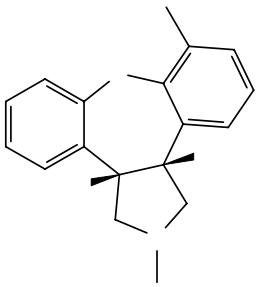

77

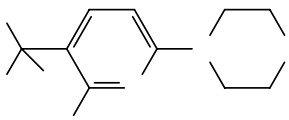

78

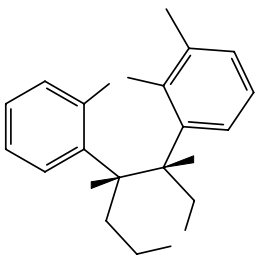

79

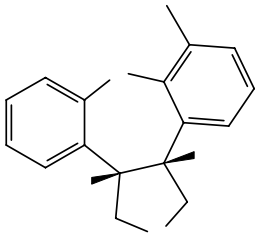

80

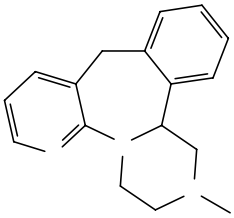

81

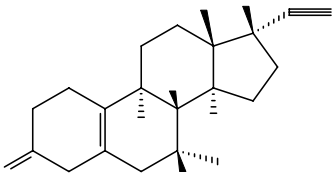

82

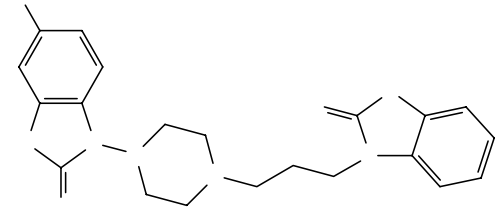

83

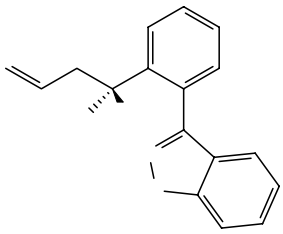

84

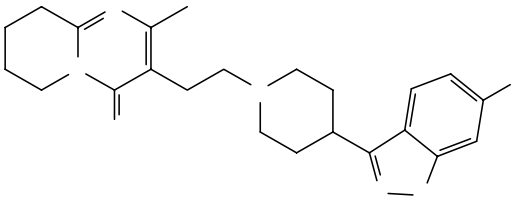

85

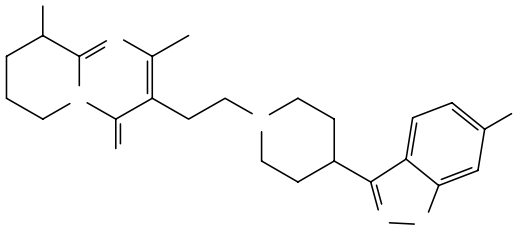

86

Figure 1. Compounds 1-30 and 61-86

Table 1. Experimental and calculated log*BB* values for the training set compounds and their computed descriptors

Compound	*V* (nm^3)	*PSA* (nm^2)	log*BB*		
			Exp.[a]	Calc.[b]	Pred.[c]

1		0.3097	0.9784	-1.42	-1.02	-0.99
2		0.1735	0.7807	-0.04	-	-
3		0.5088	0.8774	-1.06	-1.05	-1.05
4		0.3812	0.3011	0.49	0.52	0.53
5		0.3828	0.0540	0.83	1.08	1.10
6		0.3488	1.4402	-0.82	-	-
7		0.3424	0.8425	-0.67	-0.68	-0.68
8		0.3169	0.8517	-0.66	-0.72	-0.73
9		0.4313	0.8171	-0.12	-0.69	-0.71
10		0.2418	0.7636	-0.18	-0.69	-0.71
11		0.2516	1.0403	-1.15	-1.28	-1.29
12		0.3016	1.0698	-1.57	-1.23	-1.20
13		0.3420	1.3859	-1.54	-1.89	-1.95
14		0.3902	0.9170	-0.27	-0.86	-0.88
15		0.3897	0.9412	-0.28	-0.91	-0.93
16		0.3941	0.4831	-0.46	0.11	0.13
17		0.4633	0.4442	-0.24	0.07	0.09
18		0.3383	0.3815	-0.02	0.34	0.36
19		0.4327	0.3664	0.69	0.32	0.30
20		0.4219	0.3753	0.44	0.32	0.31
21		0.4773	0.3608	0.14	0.22	0.22
22		0.4654	0.5428	0.22	-0.15	-0.18
23		0.4736	0.9747	-2.00	-1.14	-1.08
24		0.5482	0.7260	-1.30	-0.89	-0.77
25		0.2404	0.4206	0.11	0.07	0.07
26		0.3875	0.8629	-1.12	-0.73	-0.72
27		0.5010	0.8539	-0.73	-0.97	-0.99
28		0.2415	0.9040	-1.17	-1.00	-0.99
29		0.3882	0.8955	-1.23	-0.81	-0.79
30		0.3562	0.7315	-2.15	-	-
31	butanone	0.1164	0.1998	-0.08	-0.04	-0.04
32	benzene	0.1147	0.0000	0.37	0.40	0.40
33	3-methylpentane	0.1597	0.0000	1.01	0.67	0.65
34	3-methylhexane	0.1828	0.0000	0.90	0.78	0.78
35	2-propanol	0.0989	0.2311	-0.15	-0.23	-0.23
36	2-methylpropanol	0.1223	0.2201	-0.17	-0.05	-0.04
37	2-methylpentane	0.1608	0.0000	0.97	0.67	0.66
38	2,2-dimethylbutane	0.1587	0.0000	1.04	0.66	0.65
39	1□1□1-trifluoro-2-chloroethane	0.1009	0.0000	0.08	0.30	0.32
40	1,1,1-trichloroethane	0.1237	0.0000	0.40	0.46	0.46
41	diethyl ether	0.1272	0.1052	0.00	0.24	0.25
42	enflurane	0.1446	0.0918	0.24	0.38	0.38
43	ethanol	0.0760	0.2421	-0.16	-0.42	-0.45
44	fluroxene	0.1311	0.1104	0.13	0.25	0.26

45	halothane	0.1273	0.0000	0.35	0.48	0.48
46	heptane	0.1857	0.0000	0.81	0.80	0.79
47	hexane	0.1630	0.0000	0.80	0.68	0.68
48	isoflurane	0.1444	0.1003	0.42	0.36	0.35
49	methylcyclopentane	0.1460	0.0000	0.93	0.59	0.58
50	pentane	0.1388	0.0000	0.76	0.55	0.54
51	propanol	0.0995	0.2417	-0.16	-0.24	-0.25
52	propanone	0.0932	0.2201	-0.15	-0.24	-0.25
53	teflurane	0.1141	0.0000	0.27	0.39	0.40
54	toluene	0.1389	0.0000	0.37	0.55	0.55
55	trichloroethene	0.1136	0.0000	0.34	0.39	0.39
56	acetylsalicylic acid	0.2048	0.6940	-0.50	-0.67	-0.68
57	valproic acid	0.2155	0.4233	-0.22	-0.02	-0.02
58	salicylic acid	0.1522	0.6312	-1.10	-0.78	-0.77
59	p-acetamidophenol	0.1817	0.5959	-0.31	-0.55	-0.56
60	chlorambucil	0.3575	0.4884	-1.70	-	-
61		0.2477	0.4004	-1.30	-	-
62		0.2051	0.4765	-1.40	-	-
63		0.3696	0.6736	-0.43	-0.30	-0.30
64		0.3624	0.4342	0.25	0.23	0.23
65		0.1936	0.2813	-0.30	0.20	0.22
66		0.2164	0.1880	-0.06	0.51	0.52
67		0.1560	0.4216	-0.42	-0.30	-0.29
68		0.3755	0.4031	-0.16	0.30	0.32
69		0.2763	0.4667	0.00	0.07	0.07
70		0.2858	0.6592	-0.34	-0.34	-0.34
71		0.3981	0.7959	-0.30	-0.59	-0.60
72		0.4053	1.0088	-1.34	-1.07	-1.06
73		0.4124	1.2201	-1.82	-1.56	-1.53
74		0.3774	0.0560	0.89	1.07	1.09
75		0.3425	0.0839	0.99	1.01	1.01
76		0.3619	0.3054	0.82	0.52	0.51
77		0.3435	0.3384	1.03	0.44	0.42
78		0.2698	0.2965	1.64	-	-
79		0.3373	0.4139	0.52	0.27	0.26
80		0.3184	0.4533	0.39	0.17	0.16
81		0.3379	0.2052	0.53	0.74	0.75
82		0.4110	0.4138	0.40	0.25	0.24
83		0.4774	0.8300	-0.78	-0.83	-0.83
84		0.3254	0.5289	0.00	0.01	0.01
85		0.4932	0.6306	-0.02	-0.44	-0.47
86		0.5010	0.8453	-0.67	-0.95	-0.98

a From references [2, 6-8, 17-20]

b Calculated from Equation 1

c Predicted using the leave-one-out cross validation procedure

Using *PSA* and *V* as regression variables, the following regression equation is obtained from the stepwise multiple regression analysis (including quadratic terms) for the 86 compounds,

$$\log BB = -13.31V^2 + 9.601V - 2.231PSA - 0.5290$$

$$n=79 \quad r^2=0.83 \quad q^2=0.82 \quad s=0.31 \quad F=126 \qquad (1)$$

where n is the number of compounds, r is the correlation coefficient, q is the cross validation coefficient, s is the standard deviation, F is the Fisher F-statistic. Compounds 2, 6, 30, 60, 61, 62 and 78 are removed from above equation as outliers. The calculated log*BB* values for the training set are presented in Table 1 and the experimental and calculated log*BB* values are plotted in Figure 2.

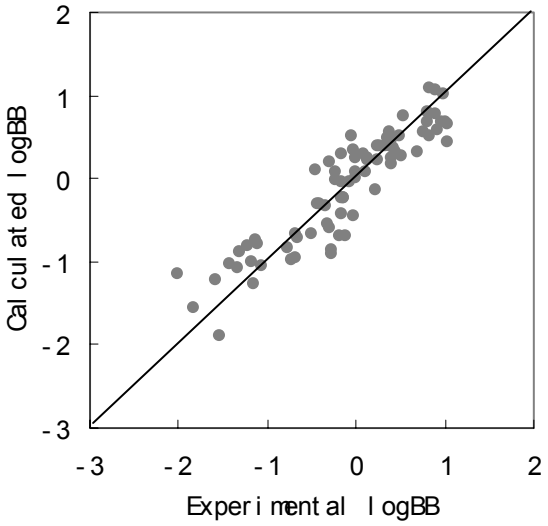

Figure 2 Relationship between experimental and calculated log*BB* values for the training set

Equation 1 displays good statistical significance. As shown in Table 1 and Figure 2, the calculated log*BB* values are in good agreement with respective experimental ones. The log*BB* value of a compound is correlated with its molecular size parabolically and its polar surface area inversely.

Because the polar surface area is a descriptor of hydrogen-bonding potential [25], Equation 1 indicates that the log*BB* of a compound is inversely correlated with its hydrogen-bonding capacity.

Equation 1 shows the parabolic relation between log*BB* and molecular volume. The explicit descriptor for lipophilicity is absent from Equation 1 and the molecular volume terms in the equation represent a combination of the impacts of molecular size and lipophilicity on BBB penetration. Increasing molecular volume decreases molecular diffusion through a lipid membrane and therefore decreases log*BB* value. On the other hand, bigger molecular volume also means higher lipophilicity which facilitates BBB penetration.

3.2 Model Validation Using the Leave-One-Out Procedure

The predictive model, Equation 1, is validated using leave-one-out procedure. Its cross validation coefficient (q^2=0.82) is almost same as its correlation coefficient (r^2=0.83). The predicted values using the leave-one-out cross validation procedure (shown in Table 1) are also very close to the respective calculated values from Equation 1. The predictive model appears to be reliable and robust.

3.3 Model Validation Using Test Set outside the Training Set

In order to assess the predictive power of Equation 1 further, a test set of log*BB* values are predicted. The experimental and predicted log*BB* values are listed in Table 2 and plotted in Figure 3.

Table 2. Experimental and calculated log*BB* values for the test set compounds and their computed descriptors

Compound		*V* (nm^3)	*PSA* (nm^2)	log*BB*			
				Exp.[a]	Pred.[b]	Pred.[c]	Pred.[d]
87	theophylline	0.1993	0.7688	-0.29	-0.86	-1.43	-0.512
88	caffeine	0.2253	0.6075	-0.06	-0.40	-1.03	-0.219
89	antipyrine	0.2357	0.2728	-0.10	0.39	-0.03	0.474
90	ibuprofen	0.2816	0.4133	-0.18	0.20	-0.09	-0.555
91	codeine	0.3596	0.4836	0.55	0.12	-0.75	0.271
92	pentobarbital	0.2822	0.8646	0.12	-0.81	-0.77	-0.191
93	alprazolam	0.3467	0.4675	0.04	0.16	-0.58	0.332
94	indomethacin	0.3988	0.7630	-1.26	-0.52	-1.07	-1.032
95	oxazepam	0.3072	0.6951	0.61	-0.39	-0.70	-0.476
96	hydroxyzine	0.4674	0.4264	0.39	0.10	-0.20	0.128
97	desipramine	0.3769	0.0932	1.20	0.99	0.77	0.426
98	midazolam	0.3677	0.3206	0.36	0.49	-0.02	0.400
99	verapamil	0.5994	0.6787	-0.70	-1.07	-1.32	-1.111
100	promazine	0.3607	0.0834	1.23	1.02	0.78	0.832
101	chlorpromazine	0.3788	0.0831	1.06	1.01	0.86	0.710
102	trifluoroperazine	0.3944	0.0948	1.44	0.98	0.70	0.459
103	thioridazine	0.4579	0.0698	0.24	0.92	0.89	1.062
104	BCNU	0.2258	0.6703	-0.52	-0.54	-0.56	-0.570
105	phenserine	0.4191	0.4825	1.00	0.08	-0.23	0.230
106	physostigmine	0.3514	0.5167	0.08	0.05	-0.50	0.007
107	terbutylchlorambucil	0.4528	0.2624	1.00	0.50	0.28	-0.227

108 didanosine	0.2625	1.0139	-1.30	-1.19	-1.95	-0.816
109 zidovudine	0.2941	1.3735	-0.72	-1.92	-2.37	-1.024
110 nevirapine	0.3132	0.5732	0.00	-0.11	-0.95	-0.285
111 SB-222200	0.4817	0.4306	0.30	0.05	0.19	0.426

a From references [17-18, 21-22]

b Predicted from Equation 1

c Predicted from the model developed by Feher et al.[12]

d Predicted from the model developed by Luco [11]

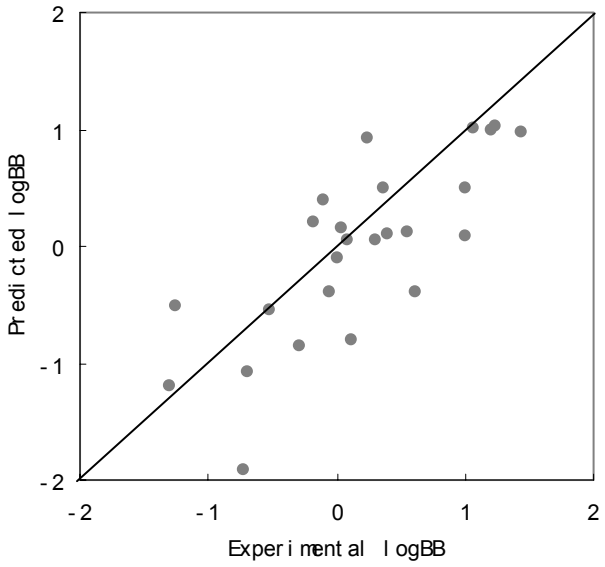

Figure 3 Relationship between experimental and predicted log*BB* values for the test set

As may be seen from Table 2 and Figure 3, the predicted log*BB* values from Equation 1 are in good agreement with the respective experimental ones and only four compounds (92, 95, 105, and 109) are predicted above or near three standard deviations. The RMSE value calculated on the 25 validation compounds is 0.53. Considering the experimental difficulties and the varied experimental conditions under which the log*BB* values have been obtained, the predictive model for BBB penetration only containing molecular volume and polar surface area performs reasonably well.

As shown in Table 2, these prediction results are superior to the one obtained by the model reported by Feher et al. (RMSE= 0.79) [12] and as good as the three-component model based on 25 descriptors using the multivariate partial least-squares procedure (RMSE=0.54) [11]. However, our model is much simpler than the three-component model [11], so more suitable for the rapid prediction of the BBB penetration for a wide range of drug candidates.

4 CONCLUSIONS

The model derived in this paper for the prediction of BBB penetration shows a good predictive power. It contains only two descriptors, namely molecular volume and polar surface area which can be easy to interpret and compute. The model appears to be very simple but robust and effective for predictive use, so it is suitable for the rapid prediction of the BBB penetration for a wide range of drug candidates.

5 REFERENCES

[1] W.M. Pardridrge, L.J. Mietus, Transport of steroid hormones through the rat blood-brain barrier, *J. Clin. Invest.* **1979**, *64,* 145-154.

[2] R.C. Young, R.C. Mitchell, T.H. Brown, C.R. Ganellin, R. Griffiths, M. Jones, K.K. Rana, D. Saunders, I.R. Smith, N.E. Sore, T.J. Wilks, Development of a new physicochemical model for brain penetration and its application to the design of centrally acting H_2 receptor histamine antagonists, *J. Med. Chem.* **1988**, *31,* 656-671.

[3] E.G. Chikhale, K.Y. Ng, P.S. Burton, R.T. Borchardt, Hydrogen bonding potential as a determinant of the in vitro and in situ blood-brain barrier permeability of peptides, *Pharm. Res.* **1994**, *11,* 412-419.

[4] H.H. Sveigaard, L. Dalgaard, Evaluation of blood-brain barrier passage of a muscarine M1 agonist and a series of analogous tetrahydropyridines measured by in vivo microdialysis, *Pharm. Res.* **2000**, *17,* 70-76.

[5] H. van de Waterbeemd, M. Kansy, Hydrogen bonding capacity and brain penetration, *Chimia* **1992**, *46,* 299-303.

[6] J.A.D. Calder, C.R. Ganellin, Predicting the brain-penetraing capability of histaminergic compounds, *Drug Des. Discov.* **1994**, *11,* 259-268.

[7] M.H. Abraham, H.S. Chadha, R.C. Michell, Hydrogen bonding. 33. Factors that influence the distribution of solutes between blood and brain, *J. Pharm. Sci.* **1994**, *83,* 1257-1268.

[8] F. Lombardo, J.F. Blake, W.J. Curatolo, Computation of brain-blood partitioning of organic solutes via free energy calculation, *J. Med. Chem.* **1996**, *39,* 4750-4755.

[9] U. Norinder, P. Sjoberg, T. Osterberg, Theoretical calculation and prediction of brain-blood partitioning of organic solutes using Molsurf parameterization and PLS statistics, *J. Pharm. Sci.* **1998**, *87,* 952-959.

[10] D.E. Clark, Rapid calculation of polar surface area and its application to the prediction of transport phenomena. 2. Prediction of blood-brain barrier penetration, *J. Pharm. Sci.* **1999**, *88,* 815-821.

[11] J.M. Luco, Prediction of the brain-blood distribution of a large set of drugs from structurally derived descriptors using partial least-squares (PLS) modeling, *J. Chem. Inf. Comput. Sci.* **1999**, *39,* 396-404.

[12] M. Feher, E. Sourial, J.M. Schmidt, A simple model for the prediction of blood-brain partitioning, *Int. J. Pharm.* **2000**, *201,* 239-247.

[13] P. Crivori, G. Cruciani, P. Carrupt, B. Testa, Predicting blood-brain barrier permeation from three-dimensional molecular structure, *J. Med. Chem.* **2000**, *43,* 2204-2216.

[14] Y.N. Kaznessis, M.E. Snow, C.J. Blankley, Prediction of blood-brain portioning using Monte Carlo simulations of molecules in water, *J. Comput. Aid. Mol. Des.* **2001**, *15,* 697-708.

[15] K. Rose, L.H. Hall, Modeling blood-brain barrier partitioning using the electropological state, *J.*

Chem. Inf. Comput. Sci. **2002**, *42,* 651-666.

[16] F. Ooms, T. Weber, P.A. Carrupt, B. Testa, A simple model to predict blood-brain barrier permeation from 3D molecular fields, *Biochim. Biophys. Acta* **2002**, *1587,* 118-125.

[17] T. Salminen, A. Pulli, J. Taskinen, Relationship between immobilized artificial membrane chromatographic retention and the brain penetration of structurally diverse drug, *J. Pharmaceut. Biomed. Anal.* **1997**, *15,* 469-477.

[18] N.H. Greig, A. Brossi, X.F. Pei, D.K. Ingram, T.T. Soncrant, Designing Drugs for Optimal Nervous System Activity; In: *New concepts of a blood-brain barrier,* Eds. J. Greenwood, D.J.Begley, M.B. Swgal, Plenum, New York, **1995**, pp. 251-264.

[19] M.H. Abraham, H.S. Chadha, R.C. Michell, Hydrogen bonding. Part 36. Determination of blood brain distribution using octanol-water partition coefficients, *Drug Des. Discov.* **1995**, *13,* 123-131.

[20] J. Kelder, P.D.J. Grootenhuis, D.M. Bayada, L.P.C. Delbressine, J.P. Ploemen, Polar molecular surface as a dominating determinant for oral absorption and brain penetration of drugs, *Pharm. Res.* **1999**, *16,* 1514-1519.

[21] A. von Sprecher, M. Gerpacher, G.P. Anderson, Neurokinin antagonists as potential therapies for inflammation and rheumatoid arthritis, *IDrugs* **1998**, *1,* 73-91.

[22] M. Yazdanian, S.L. Glynn, In vitro blood-brain barrier permeability of nevirapine compared to other HIV antiretroviral agents, *J. Pharm. Sci.* **1998**, *87,* 306-310.

[23] M.J.S. Dewar, G.E. Zoebisch, E.F. Healy, J.J.P. Stewart, AM1: A new general purpose quamtum mechanical molecular model, *J. Am. Chem. Soc.* **1985**, *107,* 3902-3909.

[24] S. Wold, Cross-Validatory Estimation of the Number of Components in Factor and Principal Component Models, *Technometrics* **1978**, *20,* 397-406.

[25] P. Stenberg, U. Norinder, K. Luthman, P. Artursson, Experimental and Computational Screening Models for the Prediction of Intestinal Drug Absorption, *J. Med. Chem.* **2001**, *44,* 1927-1937.